Factors controlling the configuration of the fresh–saline water interface in the Dead Sea coastal aquifers: synthesis of TDEM surveys and numerical groundwater modeling

Y. Yechieli · U. Kafri · M. Goldman · C. I. Voss

Abstract TDEM (time domain electromagnetic) traverses in the Dead Sea (DS) coastal aquifer help to delineate the configuration of the interrelated fresh-water and brine bodies and the interface in between. A good linear correlation exists between the logarithm of TDEM resistivity and the chloride concentration of groundwater, mostly in the higher salinity range, close to that of the DS brine. In this range, salinity is the most important factor controlling resistivity. The configuration of the fresh–saline water interface is dictated by the hydraulic gradient, which is controlled by a number of hydrological factors.

Three types of irregularities in the configuration of fresh-water and saline-water bodies were observed in the study area:

1. Fresh-water aquifers underlying more saline ones ("Reversal") in a multi-aquifer system.
2. "Reversal" and irregular residual saline-water bodies related to historical, frequently fluctuating DS base level and respective interfaces, which have not undergone complete flushing. A rough estimate of flushing rates may be obtained based on knowledge of the above fluctuations. The occurrence of salt beds is also a factor affecting the interface configuration.
3. The interface steepens towards and adjacent to the DS Rift fault zone. Simulation analysis with a numerical, variable-density flow model, using the US Geological Survey's SUTRA code, indicates that interface steepening may result from a steep water-level gradient across the zone, possibly due to a low hydraulic conductivity in the immediate vicinity of the fault.

Received: 12 June 2000 / Accepted: 30 April 2001
Published online: 19 July 2001

Y. Yechieli (✉) · U. Kafri
Geological Survey of Israel, 30 Malkhei Israel St.,
Jerusalem 95501, Israel
e-mail: yechieli@mail.gsi.gov.il
Tel.: +972-2-5314236, Fax: +972-2-5380688

M. Goldman
Geophysical Institute of Israel,
P.O. Box 182, Lod 71100, Israel

C.I. Voss
US Geological Survey, 431 National Center,
Reston, Virginia 20192, USA

Résumé Des profils TDEM (time domain electromagnetic) dans l'aquifère côtier de la Mer Morte ont permis de définir les contours des masses d'eau douce et d'eau saline et de leur interface. Il existe une bonne corrélation linéaire entre le logarithme de la résistivité TDEM et la concentration en chlorure de l'eau souterraine, surtout dans la gamme des plus hautes valeurs de salinité, proches de celles de la saumure de la Mer Morte. Dans cette gamme, la salinité est le facteur le plus important contrôlant la résistivité. La configuration de l'interface eau douce – eau saline est fixée par le gradient hydraulique, qui est contrôlé par un certain nombre de facteurs hydrologiques.

Trois types d'irrégularités dans la configuration des masses d'eau douce et d'eau saline ont été observées dans la zone étudiée:

1. Des aquifères d'eau douce situés sous des aquifères plus salins (situation inverse) dans un système multicouches.
2. Des masses d'eau saline résiduelles et irrégulières et en situation inverse liées à un niveau de base de la Mer Morte historique et fréquemment fluctuant et les interfaces correspondants, qui n'ont pas été complètement évacuées. Une estimation rapide des taux d'évacuation peut être faite à partir de la connaissance des fluctuations au-dessus. La présence de niveaux de sels est également un facteur qui affecte la configuration de l'interface.
3. L'interface plonge en direction de la zone de faille du rift de la Mer Morte et en est adjacent. Une analyse de la simulation par un modèle numérique d'écoulement à densité variable, utilisant le code SUTRA du Service Géologique des États-Unis, indique que le plongement de l'interface peut résulter d'un fort gradient du niveau d'eau au travers de cette zone, probablement dû à une faible conductivité hydraulique au voisinage de la faille.

Resumen En el acuífero costero del Mar Muerto (MM), se ha empleado perfiles transversales electromagnéticos en el dominio de tiempos (EMDT) para delimitar las

 DOI 10.1007/s100400100146

masas interrelacionadas de agua dulce y salmuera y la interfaz entre ambas. Se ha obtenido una buena correlación lineal entre el logaritmo de la resistividad de los perfiles EMDT y la concentración de cloruros en las aguas subterráneas, la mayor parte de las cuales se hallan en el rango más elevado de salinidad, cercano al de la salmuera del MM. En este rango, la salinidad es el factor más importante en relación con la resistividad. La configuración de la interfaz agua dulce-agua salada está determinada por el gradiente hidráulico, que a su vez está controlado por una serie de factores hidrológicos.

Se ha observado tres tipos de irregularidades en la configuración de las masas de agua dulce y salada en la zona de estudio:

1. Existencia de acuíferos de agua dulce por debajo de acuíferos más salados ("inversión"), dentro de un sistema multi-acuífero.
2. "Inversión" y masas residuales irregulares de agua salada, relacionadas con fluctuaciones frecuentes y periódicas del nivel de base del MM y de las interfaces relativas, que no han sido lavadas completamente. Se puede estimar de forma aproximada las velocidades de lavado por medio de las fluctuaciones del nivel superior. La existencia de depósitos de sal también es un factor que afecta a la configuración de la interfaz.
3. La interfaz se hace más pendiente hacia y en torno a la zona de fallas del rift del MM. Los análisis de una simulación mediante el código numérico de densidad variable SUTRA, del Servicio Geológico de los Estados Unidos, indican que dicho incremento de pendiente puede ser debido a la existencia de un gradiente piezométrico abrupto, propiciado por la baja permeabilidad del entorno inmediato de la falla.

Keywords salt-water/fresh-water relations · time domain electromagnetic (TDEM) · Dead Sea brine · hydrological modeling · flushing

Introduction

The location of the fresh–saline water interface and its configuration is most important in coastal aquifers as a basis for optimal water management. It is even more important in the surroundings of saline, sometimes landlocked, lakes where the interface is relatively shallow compared to "normal" coastal aquifers due to the higher density of the saline (brines) water. Often, because of the absence or scarcity of boreholes, geophysical (DC resistivity, TDEM) methods are employed to detect the interface. In the Dead Sea (hereafter denoted DS) coastal aquifer where DS levels are dropping rapidly (see below), understanding of ground-water flow and salt distribution is important for both local groundwater supply and to help in the study of sinkholes that have been developing since the 1980s (Wachs et al. 2000).

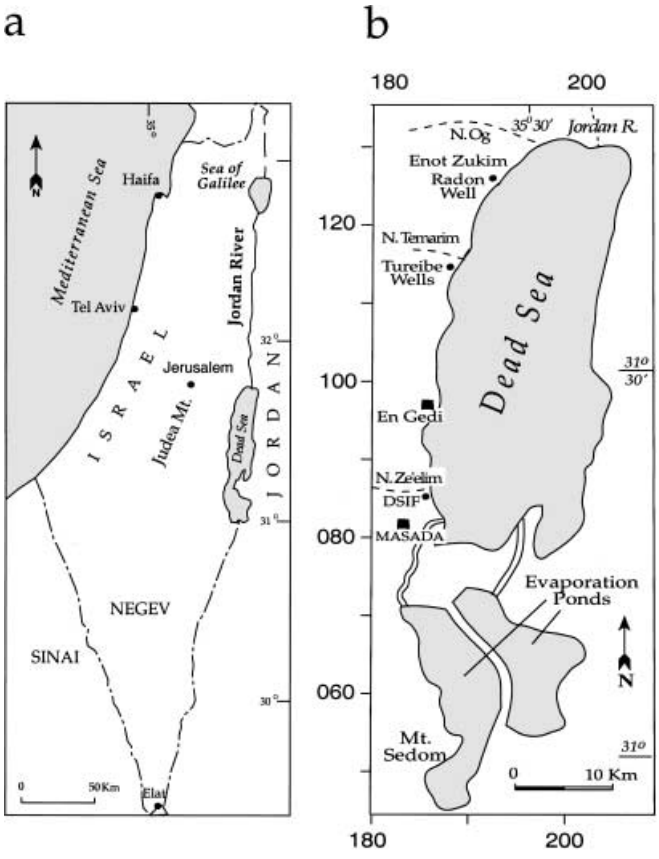

Fig. 1 Location maps: **a** general map; **b** location map of TDEM traverses (*dashed lines* at N. Og, N. Temarim and N. Ze'elim)

A fresh–saline water interface was detected in two preliminary surveys in the DS coast using electrical conductivity profiles in boreholes (Yechieli 2000) and time domain electromagnetic (TDEM) traverses (Kafri et al. 1997). The present study deals with the configuration of this interface and its irregularities, and discusses the factors and the hydrological processes that control it.

General Background

The DS is the terminal lake of the Jordan River system (Fig. 1), situated in the DS Rift, which is part of the Syrian–African Rift. The DS is known for having the lowest lake level in the world [at ~410 m b.s.l. (below sea level); deepest point in the basin is 730 m b.s.l.]. It is located in an extremely arid environment with an annual average precipitation of 70 mm. The runoff regime in this region is one of flash floods, which occur in the large wadis during the rainy winter season. The DS water is a brine with salinity of 340 g/L.

Since the early 1960s, large amounts of fresh water have been diverted from Lake Kineret (Sea of Galilee) and the Jordan River (Fig. 1), the main perennial tributary to the DS. This decrease in input of the main water source of the DS has resulted in a sharp drop in the DS

 DOI 10.1007/s100400100146

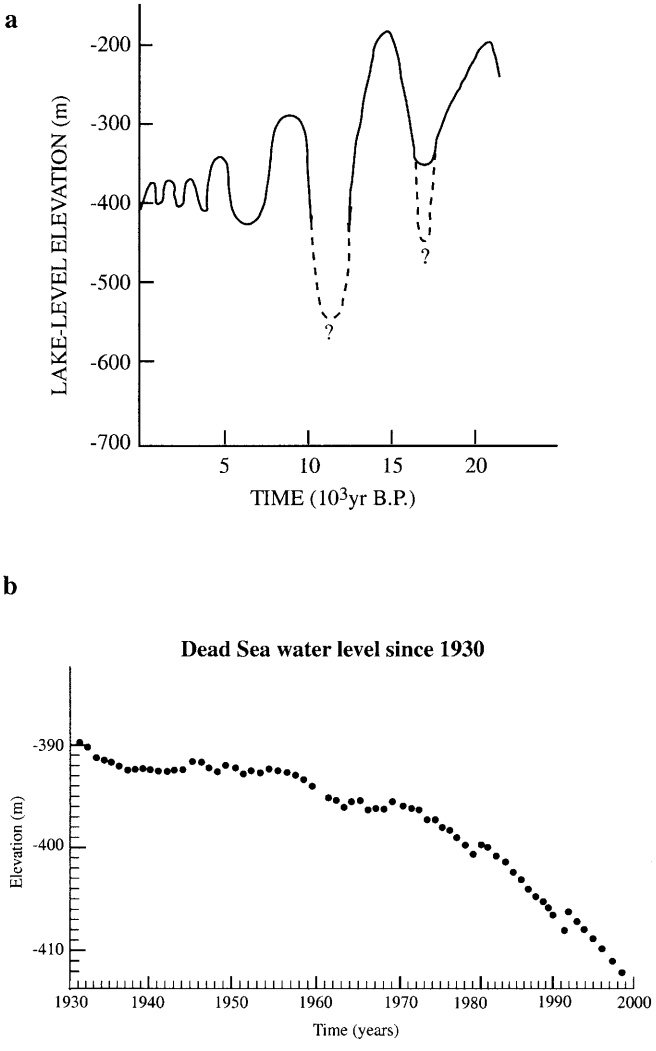

Fig. 2 Variation in DS levels: **a** in the last 20,000 years (modified after Yechieli 1993; and Frumkin et al. 1991). The high lake levels of –180m represent the level of the Lisan Lake. Fluctuations in the last 7,000 years are taken from Frumkin et al. (1991). *Dashed part of curve* and *question marks* denote a hypothetical unknown drop (not well documented) of the DS level; **b** since 1930 (modified after Klein and Flohn 1987)

level, at rates of about 0.5 m/year since the 1960s (Klein and Flohn 1987) and of 0.8 m/year in the 1980s (Anati and Shasha 1989). The decrease is expected to continue, though at a lower rate, until a new equilibrium in the water balance is reached, in about 400 years, at 100–150 m below the present level (Yechieli et al. 1998a).

Historical DS Water Levels

The changes in the lake's level, which is the regional base level, have an important bearing on the hydrological system in its vicinity. Since the Neogene, the Rift Valley was occupied by a series of lakes (Zak 1967), some of which were relatively fresh while others were extremely saline similar to the present DS. The last lake, preceding the DS, was the Lisan Lake which attained a maximal level of –180 m (Fig. 2) around 15,000 years B.P. (Druckman et al. 1987). The salinity of the Lisan Lake was probably about half that of the DS or higher (Katz et al. 1977). Later, the lake shrank to the size of the present DS and possibly smaller (Neev and Emery 1967). Since then, many small-scale fluctuations have occurred, leaving their imprint on the geohydrological scene. Evidence for these fluctuations is found on different time scales (Fig. 2): fluctuation in the Holocene has been deduced from cave records in Mt. Sedom (Frumkin et al. 1991), the sedimentary record (Kadan et al. 1995), the historical record from the last 2,000 years, and actual measurements in the last century (Klein and Flohn 1987). The drastic drop in the DS levels by some 20 m (–392 to –412 m) in the last decades is most important in understanding the hydrological regime.

Geohydrology

The major structural feature in the study area is the western border of the DS Rift, where several large normal faults exist. The coastal plain between the faults and the DS consists mainly of Quaternary continental sediments. These constitute clastics (clay, sand and gravel) deposited in fan deltas, with some intercalations of lacustrine sediments (clay, gypsum and aragonite) of the Lisan Formation (Begin et al. 1974; Sneh 1979) and younger Holocene sediments (Manspeizer 1985). The width of the coastal plain varies greatly, from about 5 km at N. Ze'elim to less than 1 km at the Enot Zukim area.

Three main aquifers are distinguished in the area surrounding the DS (Arad and Michaeli 1967; Naor et al. 1987): the deepest consists of the sandstone sequence of the Kurnub Group of Lower Cretaceous age, overlain by the limestone and dolomite sequence of the Upper Cretaceous Judea Group. The shallowest aquifer is the alluvial Quaternary aquifer which is bordered by the faults of the western margin of the DS Rift (Fig. 3). The main source of fresh-water recharge into the Quaternary aquifer is lateral flow across these faults from the Judea Group aquifer (Fig. 3), which is replenished in the mountain area some 10–30 km to the west. Flash floods in the Rift Valley also infiltrate and recharge the Quaternary aquifer. It should be noted that due to the small amount of rain which falls directly on the study area (70 mm annually) and the high evaporation, the direct recharge to groundwater is negligible.

The DS is hydraulically connected to the adjacent groundwater system, serving as a terminal base level to the groundwater flow. Therefore, the drop in the DS level is accompanied by a drop in the groundwater level (Kafri 1982; Yechieli et al. 1995). This response was found to take place within 10 d of the sharp rise in DS level in the winter of 1992 (Yechieli et al. 1995). The above changes in groundwater level are greater near the shoreline (<1 km) than at more distant points (Yechieli 1993).

 DOI 10.1007/s100400100146

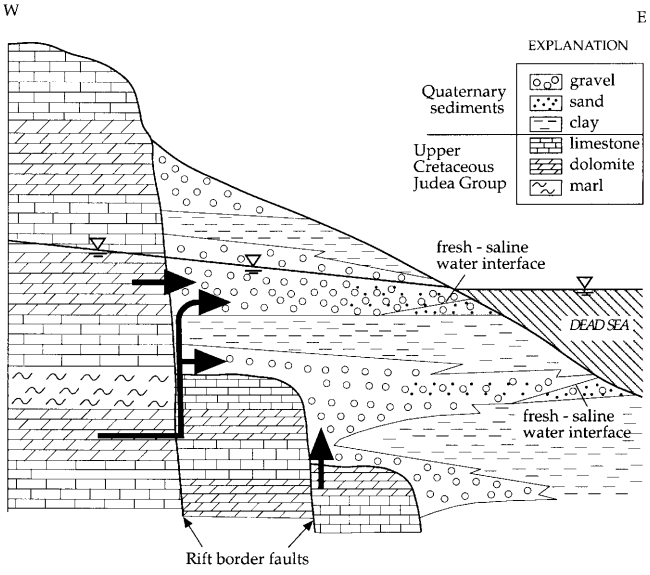

Fig. 3 Schematic cross section (not to scale) showing field relations between the different aquifers and DS. The Kurnub Group aquifer, underlying the Judea Group aquifer, is not shown. *Arrows* denote possible direction of groundwater flow. (After Yechieli et al. 1995)

The Fresh–Saline Water Interface in the DS Area

Since the density of the DS brine is 1.23 g/cc, the interface between it and the fresh groundwater is very shallow, about 10 times shallower than that found near the ocean (Yechieli 1993, 2000), following the Ghyben-Herzberg approximation for an equilibrium position. Preliminary TDEM traverses across the DS coastal plain (Kafri et al. 1997; Yechieli et al. 1998b) detected the fresh–saline water interface near the expected equilibrium position, with some deviations which are discussed below.

Method of Study

The TDEM

The time domain electromagnetic (TDEM) method, employed in this study, is described in detail by Nabighian (1979), Kaufman and Keller (1983), Fitterman and Stewart (1986) and Goldman et al. (1988) among others. Therefore, only a short description of the method, essential for understanding the hydrogeological results, is given below.

The TDEM sounding system most widely used in groundwater exploration consists of a large square transmitter (Tx) loop and a relatively small receiver (Rx) loop or multi-turn air coil placed at the Tx loop center. The Tx loop size varies between 50 by 50 m for exploration depths of up to 100 m and 500 by 500 m for a maximum depth of approximately 1,000 m. However, contrary to intuition, the Tx loop size is not a sounding parameter that controls the exploration depth as, for example, are electrode separations in standard DC resistivity methods. The Tx loop size plays a similar role to the transmitter current, i.e. it simply serves to increase signal-to-noise ratio. As far as the TDEM sounding parameter is concerned, it is the time after the Tx current has been switched off. Theoretically, the Tx current waveform can be represented by a single “step function”. However, in practice, due to technical limitations and signal-to-noise considerations, the waveform consists of a number of pulses, the shape of which depends on the instrument used (e.g. linear ramp, exponential decay, half sinusoid, etc.). The distinguishing feature of TDEM soundings is that the EM response is measured only during the Tx time-off. Thus TDEM is the only geoelectric method applied to non-polarizable targets that measures the pure secondary field caused only by induced currents and charges in the subsurface. This means that no complicated methods and tools for compensating the primary signal are necessary and, most important, the signal can be measured with short-offset arrays when the Tx/Rx separation is significantly less than the depth to the target. This feature of the TDEM methods results in excellent lateral resolution.

The transient process, which occurs after the Tx current has been switched off, can be qualitatively described as follows: at very early times, owing to the skin-effect, the induced currents are concentrated close to the Tx loop. The measured signal, consequently, is sensitive to electrical properties of shallow structures only. As the time increases, the maximum current density migrates to greater depths and the signal depends mainly on the properties of deeper layers. Thus, in addition to greater depths, the late-time measurements help to eliminate the influence of near-surface inhomogeneities (including the well-known static shift effect), often the main cause of poor data quality in other geoelectric methods, such as DC resistivity and magnetotelluric (MT).

Most of the measurements were processed and interpreted using the commercial TEMIX-XL package (Interpex 1996). The smooth (Occam’s) inversion has been first applied to each data set to choose a reasonable initial model for further layered inversion; the latter was accompanied then by a linear-sensitivity analysis. In some special cases, a global stochastic inversion has been also carried out to find essentially different solutions in the manner described in detail by Goldman et al. (1994).

An important advantage of the TDEM method is that it generally provides a narrower ambiguity range in the interpretation of the data as compared with other geoelectrical techniques. Experience gathered under various geoelectrical conditions (including both highly conductive and thick resistive targets) throughout Israel shows that interpretation errors caused by non-uniqueness of the TDEM inversion never exceeded 20–30%. At the same time, the interpretational errors caused by both poor-data quality and non-uniqueness in the DC resistivity method could be as high as several hundred percent (Goldman et al. 1988).

 DOI 10.1007/s100400100146

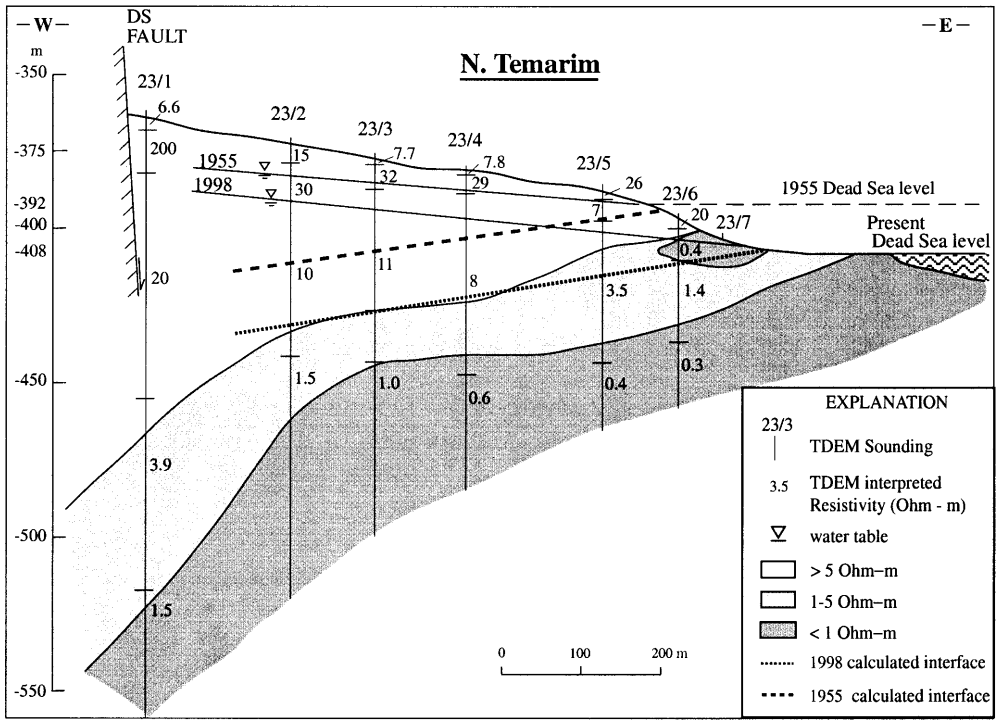

Fig. 4 TDEM traverse at N. Temarim. Location of interface was calculated according to the Ghyben-Herzberg approximation. (Modified after Kafri et al. 1997)

TDEM Applications

The TDEM method measures the resistivity of the penetrated sequence, which is mainly a combination of lithology, whether saturated or not, and the salinity of the fluids involved. It was recognized previously that most resistivities of lithologies, except for massive sulfides and graphite, vary in a wide range between a few to 100,000 ohm-m, whereas a brine has a resistivity below 1 ohm-m (Palacky 1987). Thus, very saline water can be easily distinguished from almost any lithological combination. Employing this method earlier in Israel for hydrological purposes, it was found that the method is mainly suitable for the detection of saline waters in the subsurface (Goldman et al. 1988). It was found that TDEM resistivities between 1 and 2 ohm-m are solely indicative of any lithology saturated with waters having a salinity in the range of normal seawater. TDEM resistivities below 1 ohm-m and mostly below 0.6 ohm-m, and even as low as 0.25 ohm-m, are typical of the intruding concentrated brines (sometimes partly diluted) in the DS coastal aquifer (Yechieli 1993; Kafri et al. 1997). Therefore, the above method was employed previously (Kafri et al. 1997) and in the present study to find the approximate depth and configuration of the fresh groundwater/DS brine interface. The a priori working hypothesis assumed different historical and present groundwater tables and their respective interfaces. Furthermore, for the purpose of interpreting the results from previous works, and assuming the existence of an interface between the DS brine and fresher waters, the resistivity values were subdivided into three zones: (1) resistivities above 5 ohm-m, reflecting any lithology, whether unsaturated or saturated with fresh-to-slightly brackish water, (2) resistivities below 1 ohm-m, reflecting an aquifer containing DS brine or slightly diluted DS brine, without relevance to the lithology; (3) resistivities between 1 and 2 ohm-m, reflecting salinities close to normal seawater as a result of mixing of brine with fresher groundwater.

Results

TDEM Measurements

A number of TDEM soundings have been made between the DS shore and the fault scarp (Kafri et al. 1997; Yechieli et al. 1998b). Some of the traverses show irregular configurations, possibly due to a multiple-aquifer system or to the fact that the DS system is not at a steady state because of the rapid drop of the DS base levels (discussed below). Results of three traverses are shown here. These shed light on the configuration of the different water bodies and display some interesting phenomena.

In the Nahal Ze'elim traverse (Fig. 1) the exhibited groundwater level is based on existing data. In the Temarim and Og traverses (Fig. 1), because no water-level data exist, both the present water level and the historical one (1955) are assumed and extrapolated based on base-level location and assumed hydraulic gradients. The locations of the present and the historical (1955) fresh–saline water interfaces were calculated according to the Ghyben-Herzberg approximation.

The Nahal Temarim traverse was part of a previous study (Kafri et al. 1997). The configuration of the fresh–saline water interface obtained is an "ideal" one (Fig. 4) consisting of a westward-dipping interface be-

 DOI 10.1007/s100400100146

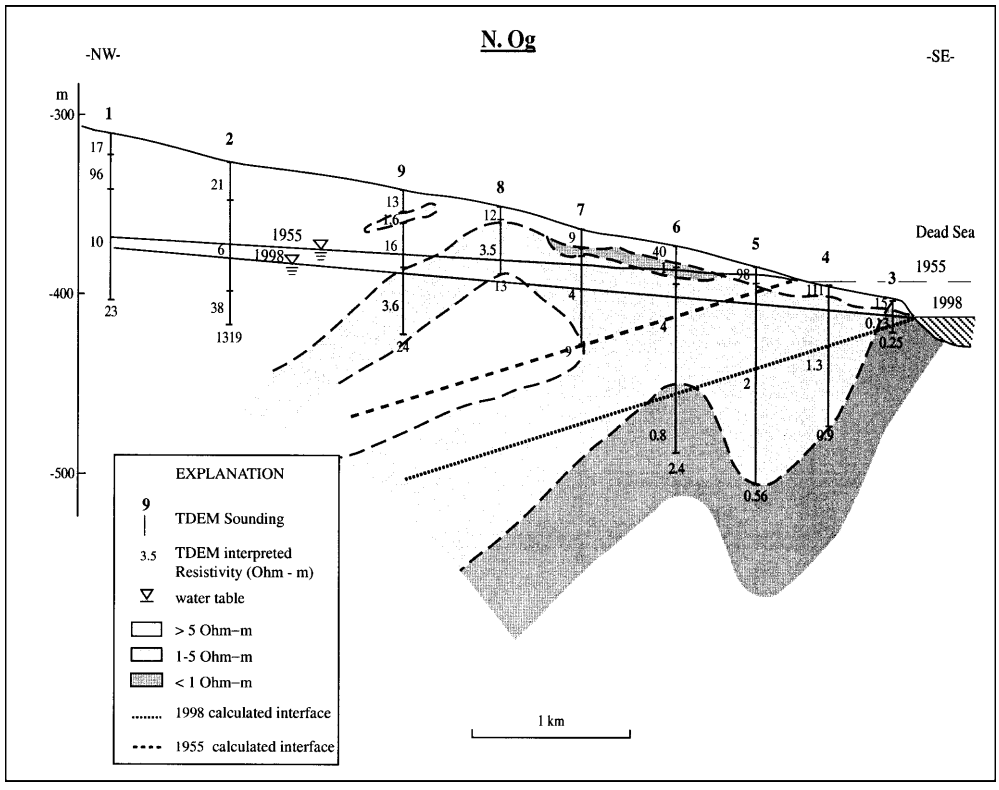

Fig. 5 TDEM traverse at N. Og. Assumed water levels and expected location of fresh–saline water interfaces are shown. Location of interface was calculated according to the Ghyben-Herzberg approximation

tween the brine and the fresh-water body and a transition (mixing) zone between them.

Two features seen in Fig. 4 commonly appear in other traverses: (1) an unflushed brine body (sounding 23/7), below and above the present water table, and (2) a steepening of the interface in the western portion of the traverse close to the fault scarp. This phenomenon is discussed separately.

The Nahal Og traverse (Fig. 5) exhibits an irregular configuration and a "reversal" of fresh water below a more saline water body. The transition (mixing) zone is thick and, as indicated in other traverses, contains unflushed brine bodies above the assumed present (1998) as well as the historical (1955) water levels.

The Nahal Ze'elim traverse (Fig. 6a) incorporates TDEM measurements with existing groundwater levels and borehole data on chloride concentration. The theoretical Ghyben-Herzberg (G-H) interfaces are calculated and shown for the present (1998) and the historical (1955) water levels. A general interface configuration with a transition zone is recognized. These are somewhat above their expected (G-H) location, indicating that the system has not yet arrived at steady state. On the other hand, the entire sequence above the water levels, except for the easternmost tip, seems to be completely flushed, exhibiting high resistivities. The phenomenon of steepening of the interface is recognized here as well, close to the fault scarp (Fig. 6b). This area coincides with a zone of steep water-level gradient caused by the drop of the water level across the fault zone (discussed below).

Hydraulic Gradients

In the particular area of the fault zone and across it, steep hydraulic-head gradients are recognized. In the Nahal Ze'elim traverse (Fig. 6b) the gradient across the main border fault, between N. Ze'elim 1 well in the Judea Group aquifer and borehole T/2 in the alluvial aquifer, is 0.038 (30 m difference in elevation along a distance of 800 m). The gradient is probably steeper in the immediate vicinity of the fault, having a step-like shape across it. Although the water levels were measured at different times (1973 and 1988 respectively), it is assumed that the gradient is indeed steep since the water level on both sides of the border faults did not change by more than a few meters. The gradient farther east, along the wide coastal plain alluvial aquifer, is an order of magnitude smaller (0.004) and a steepening close to the sea shore, between the DSIF borehole and the DS (0.01), is again recognized. A steep gradient (0.025) was also observed between the Radon well (Fig. 1) and the DS (Lang et al. 1998).

Discussion

The Relationship Between TDEM Resistivity and Groundwater Salinity

As mentioned before, the observed TDEM resistivities depend on a combination of lithology, porosity, amount of saturation, and the groundwater salinity. Unfortunately, the scarcity of TDEM and salinity data relevant to the same intervals does not enable one to obtain a correla-

 DOI 10.1007/s100400100146

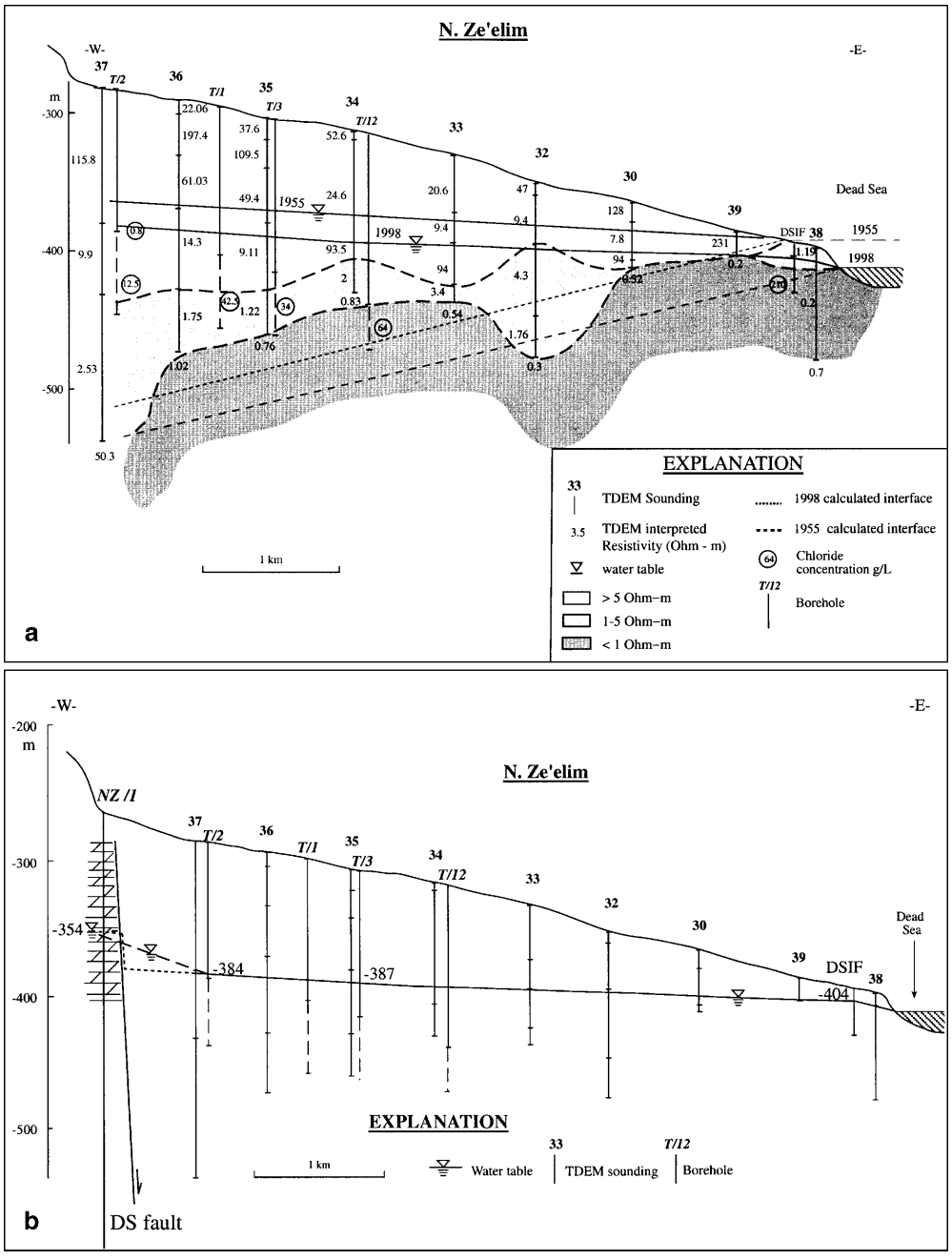

Fig. 6 **a** TDEM traverse at N. Ze'elim. The measured water level and expected location of fresh–saline water interfaces are shown. Location of interface was calculated according to the Ghyben-Herzberg approximation. **b** Water levels in N. Ze'elim, including those of the Judea Group aquifer west of the fault zone

tion between both. Resistivity values, obtained from TDEM measurements, were correlated with groundwater chloride concentrations in boreholes in the DS area, e.g. N. Ze'elim and Tureibe regions, and these data do provide a reasonable correlation (Fig. 7). It can be concluded that in the case of the higher salinities, the correlation is better, indicating that salinity of groundwater is the main factor governing the TDEM resistivity, regardless of differences in the other factors such as lithology and porosity.

Irregularity of the Fresh–Saline Water Interface

As mentioned earlier, some TDEM traverses show an irregular configuration of low-resistivity bodies and higher ones, which deviate from a conventional interface configuration. In addition, "reversals" of high resistivities (fresh water) below lower ones (saline water) are also recognized. In spite of the absence of subsurface data, and the fact that the TDEM method is unable to define a separation between the different thin sub-units, it is assumed that the above configuration is indicative of a multiple-aquifer system (Kafri et al. 1997). The DS coastal aquifer is, in most places, known to be subdivided into sub-units such as detected in the Tureibe and

 DOI 10.1007/s100400100146

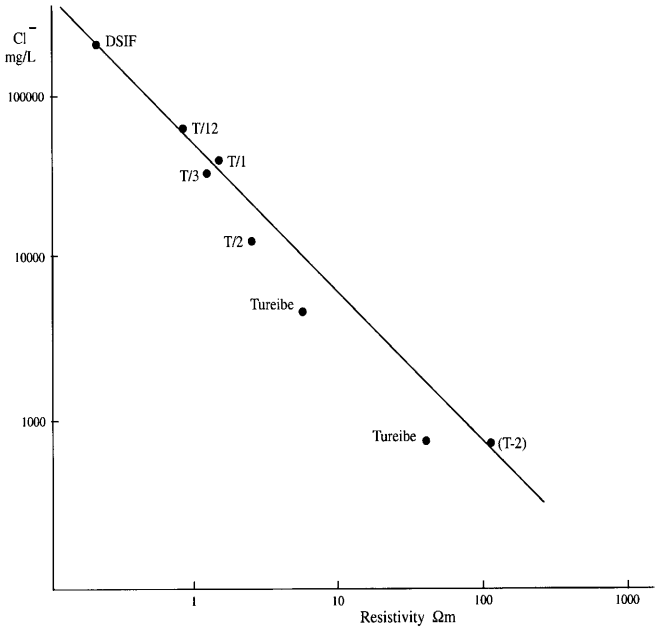

Fig. 7 Correlation between resistivity and chloride concentration of groundwater in the DS area

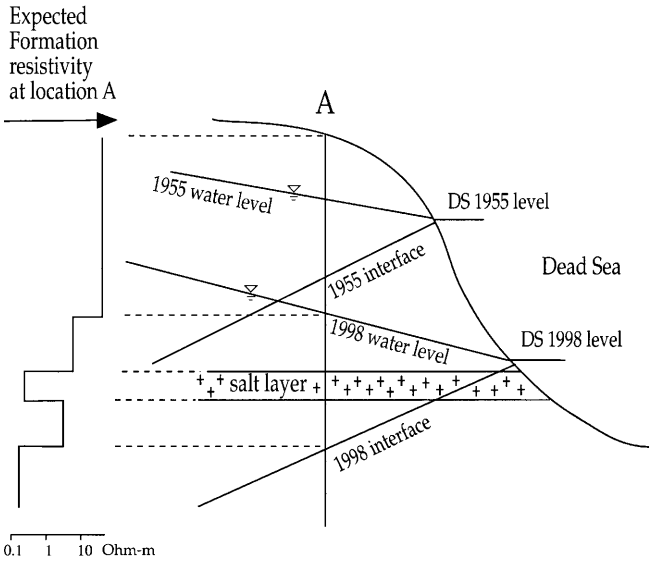

Fig. 8 Conceptual cross section of the DS coast indicating the possible effect of a salt layer on TDEM measurements. TDEM values expected at location *A* are shown at *left*

DSIF boreholes (Yechieli 1993) and the Radon boreholes (Lang et al. 1998), which are not continuous and thus defined as sub-aquifers. In such a case, it is possible that the lower fresher water is related to a different sub-aquifer, separated from the upper saline sub-aquifer.

The irregularity may also be the result of the fact that the DS system is not in steady-state conditions due to the continuous and rapid drop of the DS levels and subsequently of the groundwater levels. This non-steady-state situation is the reason that parts of the sequence have not yet been completely flushed, although they are presently located above the fresh–saline water interface. The same situation also prevails in the unsaturated zone in some locations.

Another factor that may contribute to the irregularity is the occurrence of rather shallow salt beds. Such a salt bed was found in Nahal Ze'elim in the DSIF borehole at an absolute elevation of –415 m (Yechieli 1993). Until the 1960s these salt beds were submerged below the interface and therefore were in equilibrium with the saturated brine in the salt layer. Following the drop in the DS level, and subsequent drop in the interface, the salt bed was exposed to fresher water and subjected to salt dissolution, as schematically shown in Fig. 8. This occurrence might be responsible for relatively high salinity within the fresher-water zone and manifested as an irregular configuration of water bodies. Interpolation of the TDEM soundings thus results in an apparent shallowing of the interface as indeed exhibited in N. Ze'elim, adjacent to the DSIF borehole (Fig. 6a), where a salt bed exists.

The Relationship Between Hydraulic Gradient and the Interface Configuration

Hydraulic head in the study area between the fault scarp and the DS base level exhibits a changing gradient. A general flow equation along a flow path is Q=KAJ=TJ, where Q is the amount of flow per unit of width (m^2/d), A is the thickness (m) of the saturated aquifer, J is the hydraulic-head gradient (m/m), K is the hydraulic conductivity (m/d), and T is the transmissivity (m^2/d).

Based on this equation, the gradient is expected to change in the study area for a number of reasons, as evidenced by the following considerations:

1. Near the DS shore, the thickness (A) of the freshwater zone above the interface gradually decreases eastward towards the DS. This is accompanied by a gradient increase since Q is constant (Fig. 9a). The velocity (v) is expected to increase shoreward for the same reason. Furthermore, the gradient increase in the immediate vicinity of the DS shore may be the result of the unsteady state of the DS level, as indicated by the fast drop of the sea (base) level during the last decades.
2. Changes in T values due to the change in K (lithological factor; Fig. 9b) cause a change in head gradient. The groundwater flow across the Rift border faults is from the Judea Group aquifer with high T values (10^2 m^2/d) to the DS coastal aquifer with lower T values (10^1 m^2/d).
3. The border fault, by itself, is expected to act partially as a barrier, forcing groundwater along the DS border faults, to discharge, in some places, as a series of springs. Owing to this fact, the lateral conductivity across the fault is expected to be low while

 DOI 10.1007/s100400100146

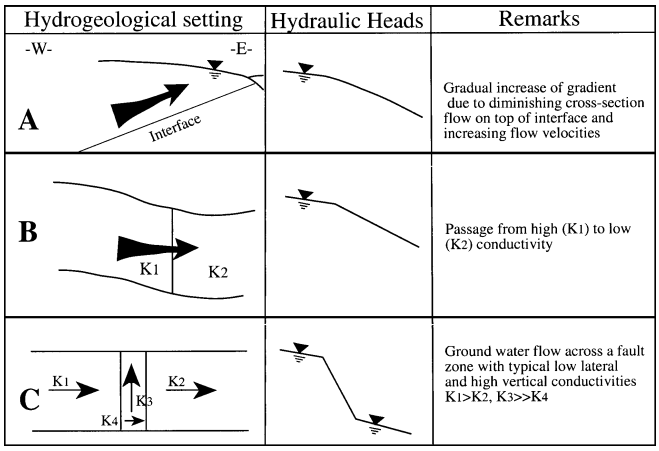

Fig. 9 Effect of different hydrogeological settings on hydraulic heads

the vertical one (parallel to the fault) may be relatively high. As a result, a large difference in head between both sides of the fault is expected (Fig. 9c), as is indeed evidenced across the border fault in Nahal Ze'elim (Fig. 6b). The steep gradient of water levels across the border faults would demand a parallel steepening of the fresh-water/brine interface. This phenomenon is indeed recognized, as mentioned above, in the N. Temarim and N. Ze'elim traverses, close to the border faults in the west (Figs. 4 and 6a).

SUTRA Simulations

The effect of the DS Rift border fault on the configuration of the interface was evaluated by simulation, using the US Geological Survey's SUTRA code (Voss 1984). Simulations generally followed the guidelines for variable-density modeling given in Voss (1999). The cross-sectional numerical simulations were done for the case of no recharge from the top, which is a reasonable assumption in this arid area, and for inflow recharge from the western boundary at a rate of 0.025 m^3/s through a strip of 1-km width from the Judea Group aquifer and across the fault zone to the alluvial aquifer; the model setup is shown in Fig. 3. The value of recharge was chosen to be in the same order of magnitude as the estimated discharge of the Zukim and Kane-Samar springs, located near Nahal Temarim. The model embodied the following conditions:

1. The mesh consisted of 1,400 elements, each 5 m deep and 40 m long.
2. Longitudinal dispersivity for horizontal flow of: α_{Lmax}=10 m; longitudinal dispersivity for vertical flow of: α_{Lmin}=1 m; transverse dispersivity of: α_T= 0.1 m.
3. Porosity of 0.2.
4. Base permeability: horizontal =5.8×10^{-12} m^2; vertical =5.8×10^{-14} m^2.

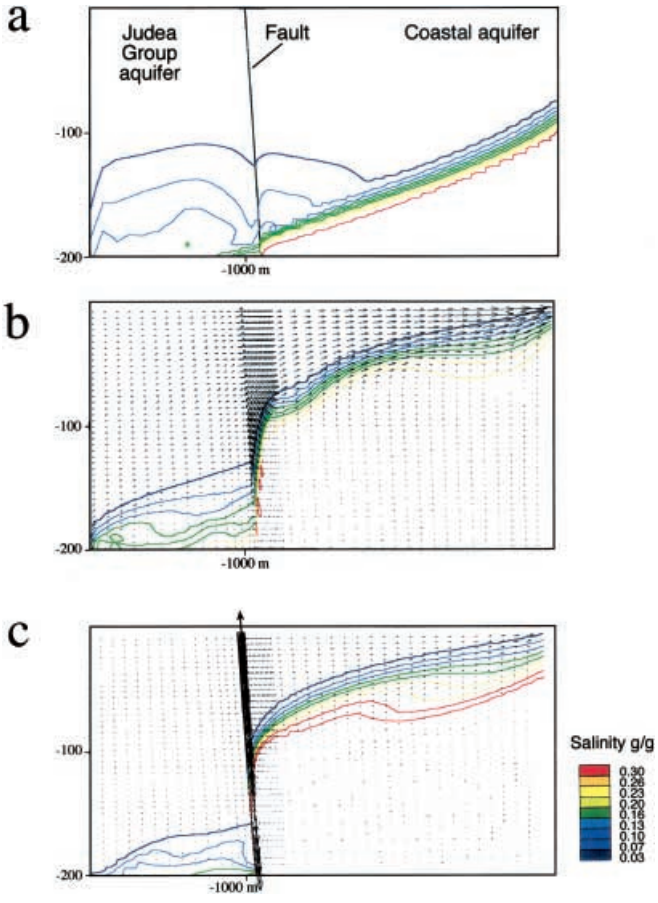

Fig. 10a–c Effect of the fault zone on configuration of the fresh–saline water interface deduced from numerical simulation with the SUTRA code. *Arrows* denote velocity vectors and *colored contours* denote salinity (in g/g). *Left* Judea Group aquifer; *right* coastal aquifer. Three simulations are shown for the following conditions: **a** passage from the higher-permeability Judea Group to the lower-permeability alluvial aquifer, with no significant permeability change assigned to the fault zone; **b** significantly lower horizontal permeability of the fault zone (horizontal conductivity of fault zone is about 200 times lower than that of the aquifers); **c** high degree of anisotropy in the fault zone in which maximal permeability is four orders of magnitude higher than the minimal value (vertical conductivity in fault zone is 10,000 times higher than horizontal conductivity). Note that maximal permeability in the fault zone is parallel to the fault dip which has a slope of 75°

5. DS-water and fresh-water density of 1.23 and 1.0 g/cc, respectively, and total dissolved solids concentration of 0.275 and 0.0 g/g (TDS=340 and 0 g/L) respectively.

The results of the steady-state simulations are shown in Fig. 10, demonstrating a change in the slope of the interface across the fault zone. Different steady-state simulations were also run for the following scenarios:

1. Higher permeability assigned for the Judea Group, changing to a lower one for the coastal alluvial aquifer at the DS fault. It was found that a difference in permeability of two orders of magnitude by itself did

 DOI 10.1007/s100400100146

not produce the steepening interface configuration near the fault as seen in the TDEM traverses (Fig. 10a). Moreover, this simulation did not produce the difference in head between both sides of the fault as was found in Nahal Ze'elim (Fig. 6b).

2. Smaller horizontal permeability (1×10^{-15} m^2, isotropic) in the fault zone, as compared to both sides of the fault. This simulation yields a better agreement (Fig. 10b) with the TDEM traverse. This simulation also produced a significant difference in head across the fault (15 m) as was indeed found in the field (Fig. 6b). Another phenomenon exhibited in this SUTRA simulation is the eastward increase of the flow velocity toward the shoreline, due to the decrease in thickness of the fresh-water portion of the aquifer.
3. Anisotropic permeability in the fault zone (four orders of magnitude higher permeability vertically along the fault as compared to the horizontal, 10^{-11} and 10^{-15} m^2). This yields the best fit with TDEM data (Fig. 10c). In this case a large head difference across the fault is exhibited, as indeed evidenced in the field in N. Ze'elim. The interface bends downwards near the fault as also shown in the TDEM traverse. In this anisotropic case there is a large vertical flow along the fault which is probably discharged as springs. Such springs indeed occur in several locations along the faults of the DS Rift. In this case the lateral flow toward the DS is smaller than in the isotropic case.

Flushing Considerations

Some 15,000 years ago, when the Lisan Lake level was at the elevation of –180 m, the entire study area of the present DS coastal plain was below lake level and thus the entire alluvial aquifer was saturated with brine. Since then, the fluctuating lake level dropped to the present DS level. As a result, the aquifer was continuously flushed by meteoric-water and lateral-groundwater inflows into the system.

The results of TDEM show that saline relicts are still found today in places above the theoretical fresh–saline water interface and sometimes even in the vadose zone. The sequence above the level of –390 m seems to be generally flushed, as expected, since it was above the DS level for a long time span, reaching steady-state conditions prior to 1955. In some cases, the rate of flushing was extremely fast, as evidenced in the N. Temarim traverse (Fig. 4). It is interesting to note that the aquifer, which only a few decades ago was saturated with DS brine when the DS level was at –390 m, is almost completely flushed following the fast drop of some 20 m in the DS level since then. Only close to the sea do saline relicts occur at –400 m, which can be attributed to the high lake level of the late 1970s. Complete flushing probably has not yet occurred due to the low hydraulic conductivity in this area. The time span for complete flushing in this area might be a few decades. Elsewhere in the study area, local saline relicts are occasionally detected at –375 m and in one case even at –350 m. These levels may be attributable to the respective lake levels which existed a few thousand to 5,000 years B.P. (Fig. 2a). Thus, it seems that in most of the area, tens of years are sufficient for an almost complete flushing of the brine following the drop of the base level. In cases of local low hydraulic conductivity, the time required for complete flushing seems to be as much as two orders of magnitude higher. The partial flushing is also undoubtedly responsible for the irregularities shown in TDEM traverses, as stated before.

Conclusions

The conclusions derived from the present study can be summarized as follows:

1. TDEM resistivities are capable of delineating water bodies of different salinities. In the range of high groundwater salinities, the salinity is the major factor governing the resistivity, as shown by the good correlation between them.
2. TDEM traverses also can delineate the configuration of water bodies of different salinities in the DS coastal aquifer and the interface between them. In some cases, an "ideal" interface configuration is indicated, while in other cases there are irregularities which may be related to a multiple-aquifer system, to non-steady state conditions, or to current dissolution of salt beds.
3. Simulations with the SUTRA code indicate that a steepening of water-table gradients, accompanied by an expected parallel steepening of the interface, as detected by the TDEM traverses, is the result of low lateral hydraulic conductivity in the DS border fault zone.
4. The flushing process of the brine from the aquifer following the base (lake) level drop is relatively rapid. In most cases, a few decades are sufficient for a complete flushing and only locally are brine relics detected at higher levels.

Acknowledgments The manuscript has greatly benefited from the constructive comments of D. Campbell and D. Fitterman. B. Cohen and N. Sheragai from the graphics department are thanked for their help. This work was funded by a grant from the Israeli Water Commission.

References

Anati AD, Shasha S (1989) Dead Sea surface level changes. Isr J Earth Sci 38:29–32

Arad A, Michaeli A (1967) Hydrogeological investigations in the western catchment of the Dead Sea. Isr J Earth Sci 16:181–196

Begin B, Ehrlich A, Nathan Y (1974) Lake Lisan, the Pleistocene precursor of the Dead Sea. Geol Surv Isr Bull 63

Druckman Y, Magaritz M, Sneh A (1987) The shrinking of Lake Lisan, as reflected by the diagenesis of its marginal oolithic deposits. Isr J Earth Sci 36:101–106

 DOI 10.1007/s100400100146

Fitterman DV, Stewart MT (1986) Transient electromagnetic sounding for groundwater. Geophysics 51:995–1005
Frumkin A, Magaritz M, Carmi I, Zak I (1991) The Holocene climatic record of the salt caves of Mount Sedom, Israel. Holocene 1(3):191–200
Goldman M, Arad A, Kafri U, Gilad D, Melloul A (1988) Detection of freshwater/seawater interface by the time domain electromagnetic (TDEM) method in Israel. Naturwet Tijdsehr 70: 339–344
Goldman M, Du Plooy A, Eckard M (1994) On reducing ambiguity in the interpretation of transient electromagnetic sounding data. Geophys Prospect 42:3–25
Interpex Ltd. (1996) TEMIX XL v4 user's manual, volumes 1 and 2. Interpex
Kadan G, Eyal Y, Enzel Y (1995) Dead Sea fluctuations and tectonic events in the Holocene fan-delta of Nahal Darga. Isr Geol Soc Meet Abstr 53
Kafri U (1982) Relationship between the Dead Sea and groundwater levels in the western Dead Sea catchment area. Geol Surv Curr Res 1981:90–94
Kafri U, Goldman M, Lang B (1997) Detection of subsurface brine, fresh water bodies and the interface configuration in between by the TDEM method in the Dead Sea Rift, Israel. Environ Geol 31:42–49
Katz A, Kolodny Y, Nissenbaum A (1977) The geochemical evolution of the Pleistocene Lake Lisan–Dead Sea system. Geochim Cosmochim Acta 41:1609–1626
Kaufman AA, Keller GV (1983) Frequency and transient soundings. Elsevier, Amsterdam, Netherlands
Klein C, Flohn A (1987) Contribution to the knowledge in the fluctuations of the Dead Sea level. Theor Appl Climatol 38: 151–156
Lang B, Kafri U, Vulcan U (1998) Radon in the unsaturated (gravel) and the saturated (groundwater) zones at the NW Dead Sea sector. Geol Surv Isr GSI/27/98
Manspeizer W (1985) The Dead Sea Rift: impact of climate and tectonism on Pleistocene and Holocene sedimentation. In: Biddle KT, Chritie-Blick N (eds) Strike slip deformation, basin formation, and sedimentation. Spec Publ 37. Society of Economic Paleontologists and Mineralogists (Society of Sedimentary Geology), Tulsa, Oklahoma, USA, pp 143–158
Nabighian M (1979) Quasi-static transient response of a conducting half-space: an approximate representation. Geophysics 44: 1700–1706
Naor H, Katz D, Harash Y (1987) Hydrogeological study to locate production wells in Wadi Zohar area (in Hebrew). Rep 04/88/28. Tahal, Tel Aviv, Israel
Neev D, Emery KO (1967) The Dead Sea. Geol Surv Isr Bull 41
Palacky GJ (1987) Resistivity characteristics of geological targets. In: Nabighian M (ed) Electromagnetic methods in applied geophysics – theory. Society of Exploration Geophysicists, Tulsa, Oklahoma, USA, pp 53–129
Sneh A (1979) Late Pleistocene fan deltas along the Dead Sea Rift. J Sediment Pet 49:541–552
Voss CI (1984) SUTRA: finite-element simulation model for saturated–unsaturated, fluid-density-dependent groundwater flow with energy transport or chemically-reactive single species solute transport. US Geol Surv Water Resour Invest 84–4369
Voss CI (1999) USGS SUTRA code – history, practical use, and application in Hawaii. In: Bear J, Cheng AH-D, Sorek S, Ouzar D, Herrera I (eds) Seawater intrusion in coastal aquifers – concepts, methods and practices. Kluwer, Boston, USA, pp 249–313
Wachs D, Yechieli Y, Shtivelman V, Itamar A, Baer G, Goldman M, Raz E, Rybakov M, Shatner U (2000) Formation of sinkholes along the Dead Sea shore – summary of findings from the first stage of research. Geol Surv Isr GSI/41/2000
Yechieli Y (1993) The effects of water level changes in closed lakes (Dead Sea) on the surrounding groundwater and country rocks. PhD Thesis, Weizmann Institute of Science, Rehovot, Israel
Yechieli Y (2000) Fresh–saline groundwater interface in the Western Dead Sea area. Groundwater 38:615–623
Yechieli Y, Ronen D, Berkovitz B, Dershovitz WS, Hadad A (1995) Aquifer characteristics derived from the interaction between water levels of a terminal lake (Dead Sea) and an adjacent aquifer. Water Resour Res 31(4):893–902
Yechieli Y, Gavrieli I, Ronen D, Berkovitz B (1998a) Will the Dead Sea die? Geology 26(8):755–758
Yechieli Y, Kafri U, Goldman M (1998b) Mapping of fresh and saline water bodies in the coastal aquifer of the Dead Sea, using TDEM method. Geol Surv Isr TR-GSI/8/98
Zak I (1967) The geology of Mount Sedom (in Hebrew with English summary). PhD Diss, Hebrew University, Jerusalem, Israel

 DOI 10.1007/s100400100146